ADVANCED ENERGY MATERIALS

Supporting Information

for *Adv. Energy Mater.,* DOI: 10.1002/aenm.202003369

Engineering the Site-Disorder and Lithium Distribution in the Lithium Superionic Argyrodite Li_6PS_5Br

Ajay Gautam, Marcel Sadowski, Michael Ghidiu, Nicolò Minafra, Anatoliy Senyshyn, Karsten Albe, and Wolfgang G. Zeier**

Supporting Information -

Engineering the Site-Disorder and Lithium Distribution in the Lithium Superionic Argyrodite Li_6PS_5Br

Ajay Gautam[a,b,$], Marcel Sadowski[c,$], Michael Ghidiu [a,b], Nicolò Minafra[d], Anatoliy Senyshyn[e], Karsten Albe[*c], Wolfgang G. Zeier[*d]

[a]*Institute of Physical Chemistry, Justus-Liebig-University Giessen, Heinrich-Buff-Ring 17, D-35392 Giessen, Germany.*

[b]*Center for Materials Research (LaMa), Justus-Liebig-University Giessen, Heinrich-Buff-Ring 16, D-35392 Giessen, Germany.*

[c]*Department of Materials Science, Technical University of Darmstadt, Otto-Berndt-Strasse 3, D-64287 Darmstadt, Germany.*

[d]*Institute of Inorganic and Analytical Chemistry, University of Münster, Correnstrasse 30, 48149 Münster, Germany*

[e]*Heinz Maier-Leibnitz Zentrum, Technische Universitaet München, 85748 Garching, Germany*

[$]*These authors contributed equally to this work*

E-mail:

*wzeier@uni-muenster.de

*albe@mm.tu-darmstadt.de

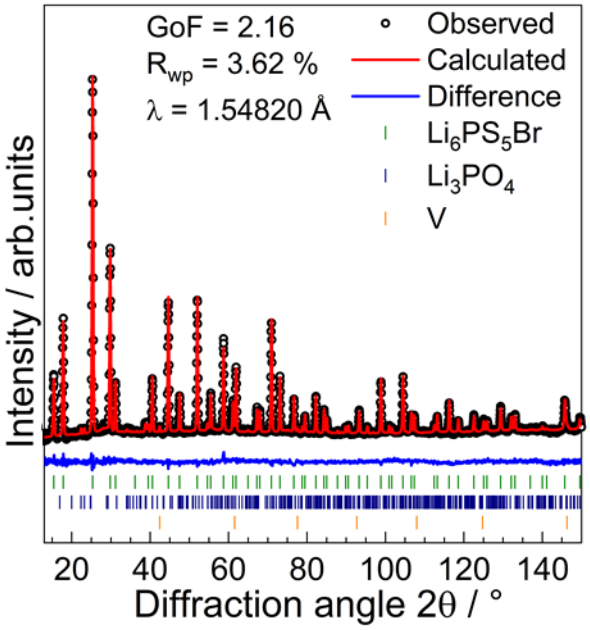

Figure S1: Neutron diffraction data and the corresponding Rietveld refinement of the slow cooled Li_6PS_5Br, that was afterwards heated at 350 ºC for 2 hours, followed by quenching. Experimental data are shown in black and the red line denotes the calculated pattern, while the difference profile is shown in blue. Calculated positions of the Li_6PS_5Br and Li_3PO_4 Bragg reflections are shown as green and blue vertical ticks; additional reflections belong to the vanadium sample holder (yellow ticks).

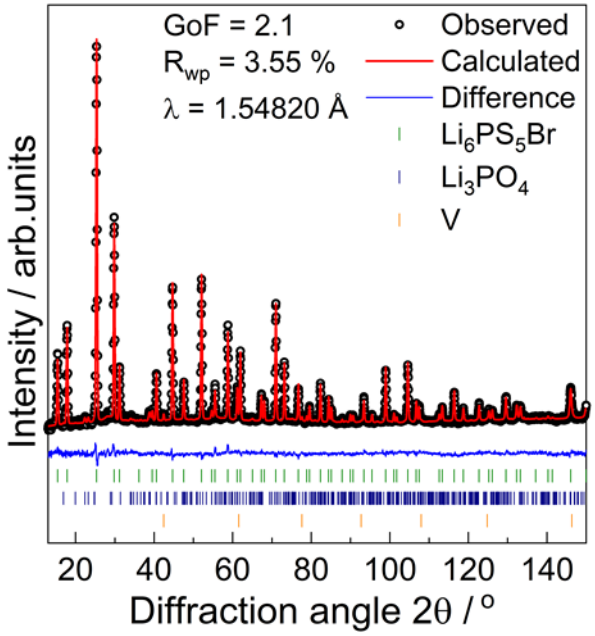

Figure S2: Neutron diffraction data and the corresponding Rietveld refinement of the slow cooled Li_6PS_5Br, that was afterwards heated at 400 ºC for 2 hours, followed by quenching. Experimental data are shown in black and the red line denotes the calculated pattern, while the difference profile is shown in blue. Calculated positions of the Li_6PS_5Br and Li_3PO_4 Bragg reflections are shown as green and blue vertical ticks; additional reflections belong to the vanadium sample holder (yellow ticks).

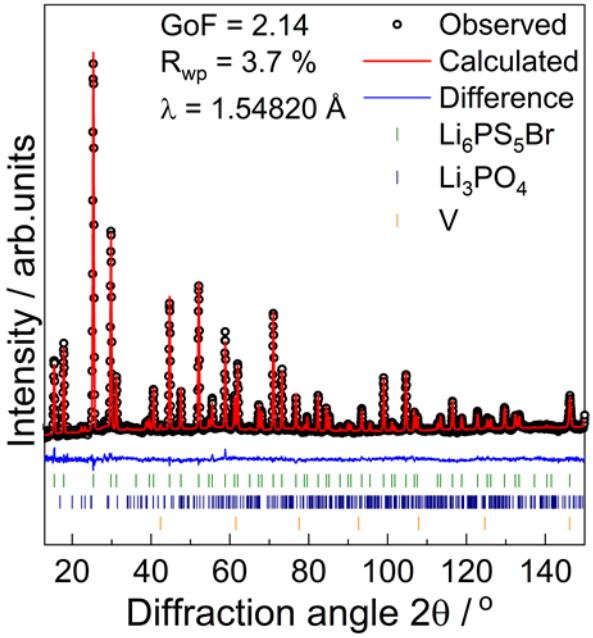

Figure S3: Neutron diffraction data and the corresponding Rietveld refinement of the slow cooled Li_6PS_5Br, that was afterwards heated at 450 ºC for 2 hours, followed by quenching. Experimental data are shown in black and the red line denotes the calculated pattern, while the difference profile is shown in blue. Calculated positions of the Li_6PS_5Br and Li_3PO_4 Bragg reflections are shown as green and blue vertical ticks; additional reflections belong to the vanadium sample holder (yellow ticks)..

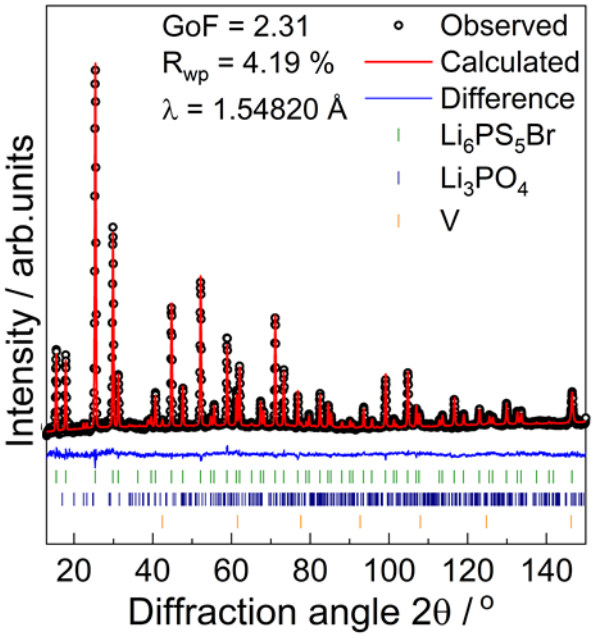

Figure S4: Neutron diffraction data and the corresponding Rietveld refinement of the slow cooled Li_6PS_5Br, that was afterwards heated at 550 ºC for 2 hours followed by quenching. Experimental data are shown in black and the red line denotes the calculated pattern, while the difference profile is shown in blue. Calculated positions of the Li_6PS_5Br and Li_3PO_4 Bragg reflections are

shown as green and blue vertical ticks; additional reflections belong to the vanadium sample holder (yellow ticks)..

Table S1. Constraints used to refine Li_6PS_5Br neutron diffraction data (all temperatures, except 550 °C).

Atom	Wyckoff site	*x/a*	y/*b*	z/*c*	Occ	B_{eq}/ Å^2
LiT5	48*h*	*Pos1*	*Pos2*	*1-Pos1*	*Occ1*	*Var1*
LiT2	48*h*	*Pos3*	*Pos4*	*0.5+Pos4*	*Occ2*	*Var2*
LiT5a	24*g*	0.25	*Pos5*	0.75	*1-2·Occ1-2·Occ2*	*Var1*
Br1	4*a*	0	0	1	*Occ3*	*Var3*
Br2	4*d*	0.25	0.25	0.75	*1-Occ3*	*Var4*
P1	4*b*	0	0	0.5	*1*	*Var5*
S1	4*d*	0.25	0.25	0.75	*Occ3*	*Var4*
S2	16*e*	*Pos6*	*-Pos6*	*0.5+Pos6*	*1*	*Var6*
S3	4*a*	0	0	1	*1-Occ3*	*Var3*

Table S2. Constraints used to refine Li_6PS_5Br (550 °C heat treatment) neutron diffraction data

Atom	Wyckoff site	*x/a*	y/*b*	z/*c*	Occ	B_{eq}/ Å^2
LiT5	48*h*	*Pos1*	*Pos2*	*1-Pos1*	*Occ1*	*Var1*
LiT2	48*h*	*Pos3*	*Pos4*	*0.5+Pos4*	*0.5-Occ1*	*Var2*
Br1	4*a*	0	0	1	*Occ2*	*Var3*
Br2	4*d*	0.25	0.25	0.75	*1-Occ2*	*Var4*
P1	4*b*	0	0	0.5	*1*	*Var5*
S1	4*d*	0.25	0.25	0.75	*Occ2*	*Var4*
S2	16*e*	*Pos5*	*-Pos5*	*0.5+Pos5*	*1*	*Var6*
S3	4*a*	0	0	1	*1-Occ2*	*Var3*

Table S3. Crystallographic data of Li_6PS_5Br of the slow cooled sample. The lattice parameter, atomic positions, occupancies, and thermal coefficient parameter are obtained from the Rietveld refinements against the neutron diffraction data. Refined parameters are shown with uncertainty in parentheses.

a = 9.99475(9) Å; 0.58 wt % Li_3PO_4 R_{wp} = 3.59 % ; GoF = 2.11 λ = 1.54820 Å						
Atom	Wyckoff site	*x/a*	y/*b*	z/*c*	Occ	B_{eq}/ Å^2
LiT5	48*h*	0.3050(5)	0.0247(6)	0.6950(5)	0.306(8)	2.6(2)
LiT2	48*h*	0.288(3)	0.074(2)	0.574(2)	0.118(9)	10(1)
LiT5a	24*g*	0.25	0.015(3)	0.75	0.15(2)	2.6(2)
Br1	4*a*	0	0	1	0.901(8)	3.34(5)
Br2	4*d*	0.25	0.25	0.75	0.098(8)	2.02(8)
P1	4*b*	0	0	0.5	1	1.75(4)
S1	4*d*	0.25	0.25	0.75	0.901(8)	2.02(8)
S2	16*e*	0.1182(1)	-0.1182(1)	0.6182(1)	1	2.31(4)
S3	4*a*	0	0	1.0	0.098(8)	3.34(5)

Table S4. Crystallographic data of slow cooled Li_6PS_5Br that was afterwards heated at 350 ºC for 2 hours, followed by quenching. The lattice parameter, atomic positions, occupancies, and thermal coefficient parameter are obtained from the Rietveld refinements against the neutron diffraction data. Refined parameters are shown with uncertainty in parentheses.

a = 9.9868(1) Å; 0.56 wt % Li_3PO_4 R_{wp} = 3.62% ; GoF = 2.16 λ = 1.54820 Å						
Atom	Wyckoff site	*x/a*	y/*b*	z/*c*	Occ	B_{eq}/ Å^2
LiT5	48*h*	0.3079(5)	0.0233(7)	0.6921(5)	0.303(9)	2.8(2)
LiT2	48*h*	0.294(2)	0.072(2)	0.572(2)	0.130(11)	12(1)
LiT5a	24*g*	0.25	0.014(3)	0.75	0.131(28)	2.8(2)
Br1	4*a*	0	0	1	0.821(6)	3.46(6)
Br2	4*d*	0.25	0.25	0.75	0.178(6)	2.14(6)
P1	4*b*	0	0	0.5	1	1.82(3)
S1	4*d*	0.25	0.25	0.75	0.821(6)	2.14(6)
S2	16*e*	0.1180(2)	-0.1180(2)	0.6180(2)	1	2.37(5)
S3	4*a*	0	0	1.0	0.178(6)	3.46(6)

Table S5. Crystallographic data of slow cooled Li_6PS_5Br that was afterwards heated at 400 ºC for 2 hours, followed by quenching. The lattice parameter, atomic positions, occupancies, and thermal coefficient parameter are obtained from the Rietveld refinements against the neutron diffraction data. Refined parameters are shown with uncertainty in parentheses.

a = 9.97978(6) Å; 0.58 wt % Li_3PO_4 R_{wp} = 3.55% ; GoF = 2.1 λ = 1.54820 Å						
Atom	Wyckoff Site	*x/a*	y/*b*	z/*c*	Occ	B_{eq}/ Å^2
LiT5	48*h*	0.3099(6)	0.0224(7)	0.6901(6)	0.315(8)	3.3(2)
LiT2	48*h*	0.289(2)	0.064(2)	0.564(2)	0.132(10)	10(1)
LiT5a	24*g*	0.25	0.0128(5)	0.75	0.105(27)	3.3(2)
Br1	4*a*	0	0	1	0.716(7)	3.31(6)
Br2	4*d*	0.25	0.25	0.75	0.283(7)	2.21(6)
P1	4*b*	0	0	0.5	1	1.87(3)
S1	4*d*	0.25	0.25	0.75	0.716(7)	2.21(6)
S2	16*e*	0.1181(2)	-0.1181(2)	0.6181(2)	1	2.46(3)
S3	4*a*	0	0	1.0	0.283(7)	3.31(6)

Table S6. Crystallographic data of slow cooled Li_6PS_5Br that was afterwards heated at 450 ºC for 2 hours, followed by quenching. The lattice parameter, atomic positions, occupancies, and thermal coefficient parameter are obtained from the Rietveld refinements against the neutron diffraction data. Refined parameters are shown with uncertainty in parentheses.

a = 9.97442(6) Å; 0.57 wt % Li_3PO_4 R_{wp} = 3.7% ; GoF = 2.14 λ = 1.54820 Å						
Atom	Wyckoff Site	*x/a*	y/*b*	z/*c*	Occ	B_{eq}/ Å^2
LiT5	48*h*	0.3133(7)	0.0217(7)	0.6867(7)	0.381(8)	5.3(2)
LiT2	48*h*	0.272(2)	0.055(2)	0.555(2)	0.079(6)	3.1(9)
LiT5a	24*g*	0.25	0.021(3)	0.75	0.077(21)	0.08(7)
Br1	4*a*	0	0	1	0.662(7)	3.3875)
Br2	4*d*	0.25	0.25	0.75	0.337(7)	2.57(5)
P1	4*b*	0	0	0.5	1	2.07(3)
S1	4*d*	0.25	0.25	0.75	0.662(7)	2.57(5)
S2	16*e*	0.1183(1)	-0.1183(1)	0.6183(1)	1	2.55(4)
S3	4*a*	0	0	1.0	0.337(7)	3.37(5)

Table S7. Crystallographic data of slow cooled Li_6PS_5Br that was afterwards heated at 550 ºC for 2 hours, followed by quenching. The lattice parameter, atomic positions, occupancies, and thermal coefficient parameter are obtained from the Rietveld refinements against the neutron diffraction data. Refined parameters are shown with uncertainty in parentheses.

a = 9.96688(5) Å; 0.4 wt % Li_3PO_4 R_{wp} = 4.19% ; GoF = 2.31 λ = 1.54820 Å						
Atom	Wyckoff Site	*x/a*	y/*b*	z/*c*	Occ	B_{eq}/ Å^2
LiT5	48*h*	0.3139(6)	0.0219(8)	0.6861(8)	0.403(8)	5.8(3)
LiT2	48*h*	0.273(2)	0.053(2)	0.553(2)	0.096(8)	3.1(8)
Br1	4*a*	0	0	1	0.606(7)	3.02(7)
Br2	4*d*	0.25	0.25	0.75	0.394(7)	2.31(6)
P1	4*b*	0	0	0.5	1	2.06(4)
S1	4*d*	0.25	0.25	0.75	0.606(7)	2.31(6)
S2	16*e*	0.1174(2)	-0.1174(2)	0.6174(2)	1	2.64(3)
S3	4*a*	0	0	1.0	0.394(7)	3.02(7)

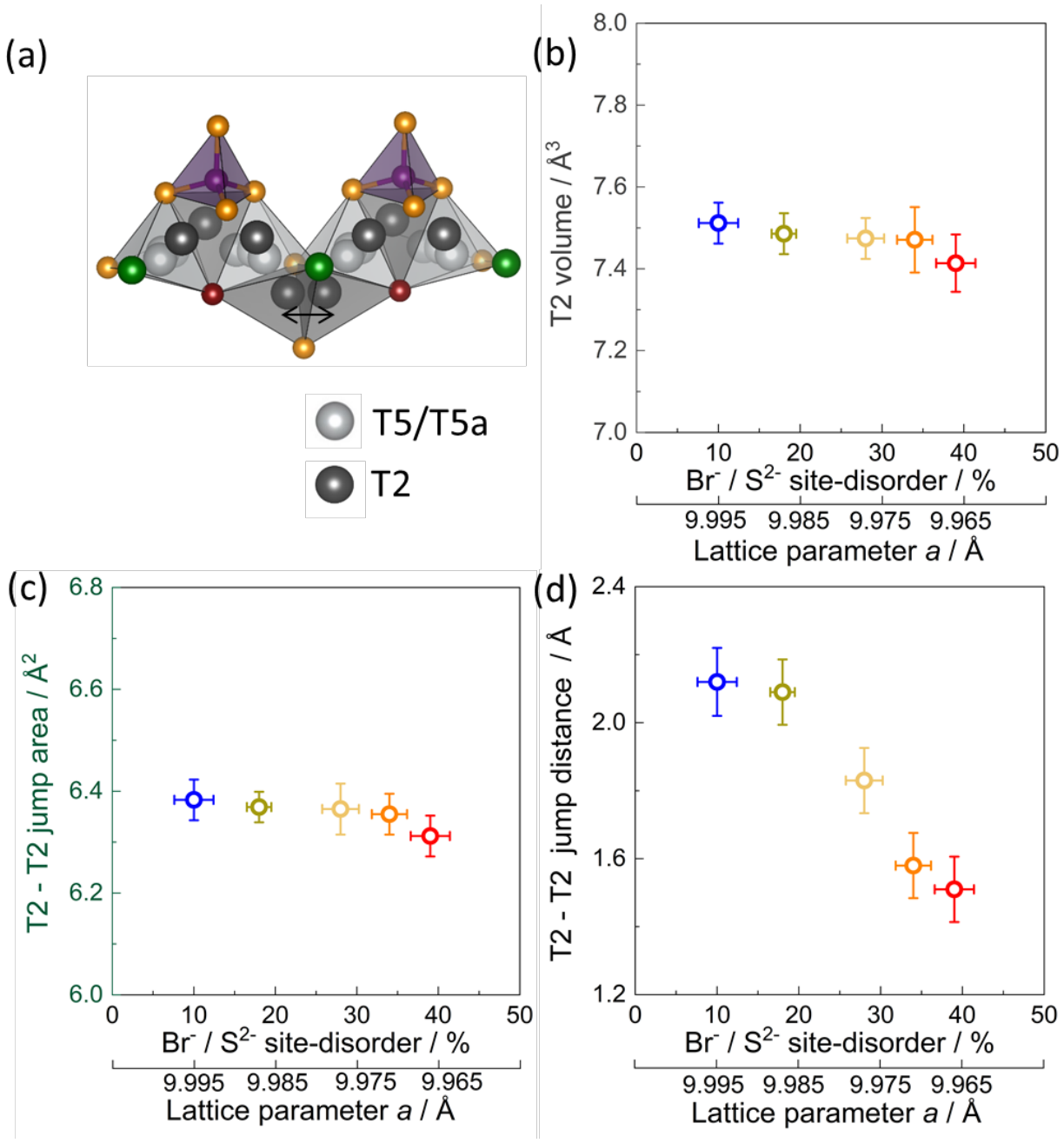

Figure S5: (a) Lithium diffusion pathways showing the tetrahedral face-connection between the T2 sites that connect the different Li^+ cages, schematic adapted from reference 1*, as well as the (b) polyhedral volumes, (c) jump areas, and (d) jump distances of the T2 site plotted against site-disorder and lattice parameter. Note the lattice parameter axis is decreasing.*

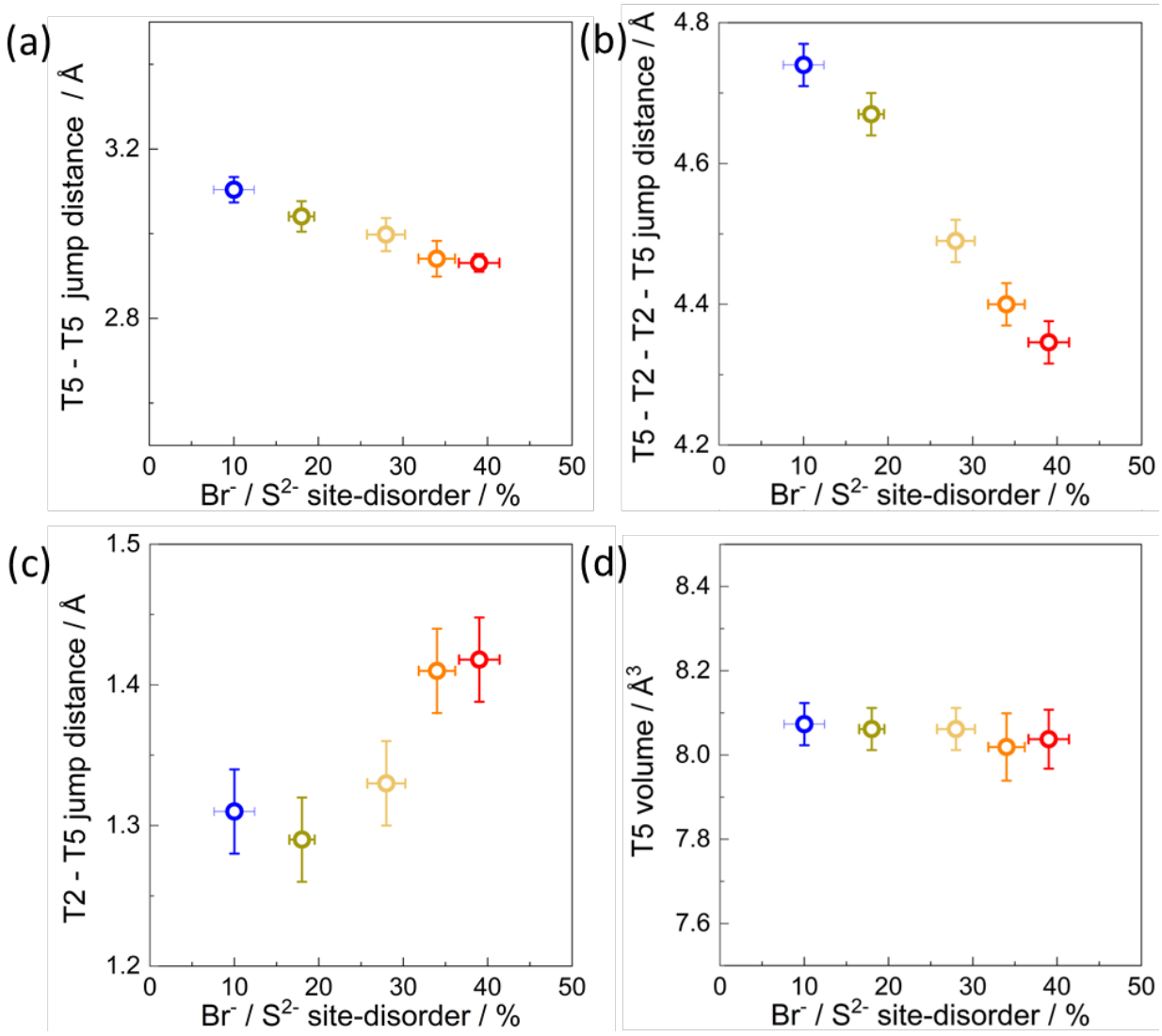

Figure S6: a) $Li^+ - Li^+$ jump distances in Li_6PS_5Br obtained from the Rietveld refinements of neutron diffraction data. With increasing site-disorder the T5 –T5 inter-cage jump distances (b) as well as the overall T5 – T2 – T2 – T5 jump distances (c) decrease, while the T2 – T5 jump distances (c) increase. d) The change on the T5 polyhedral volume as a function of the Br^-/S^{2-} site-disorder is negligible.

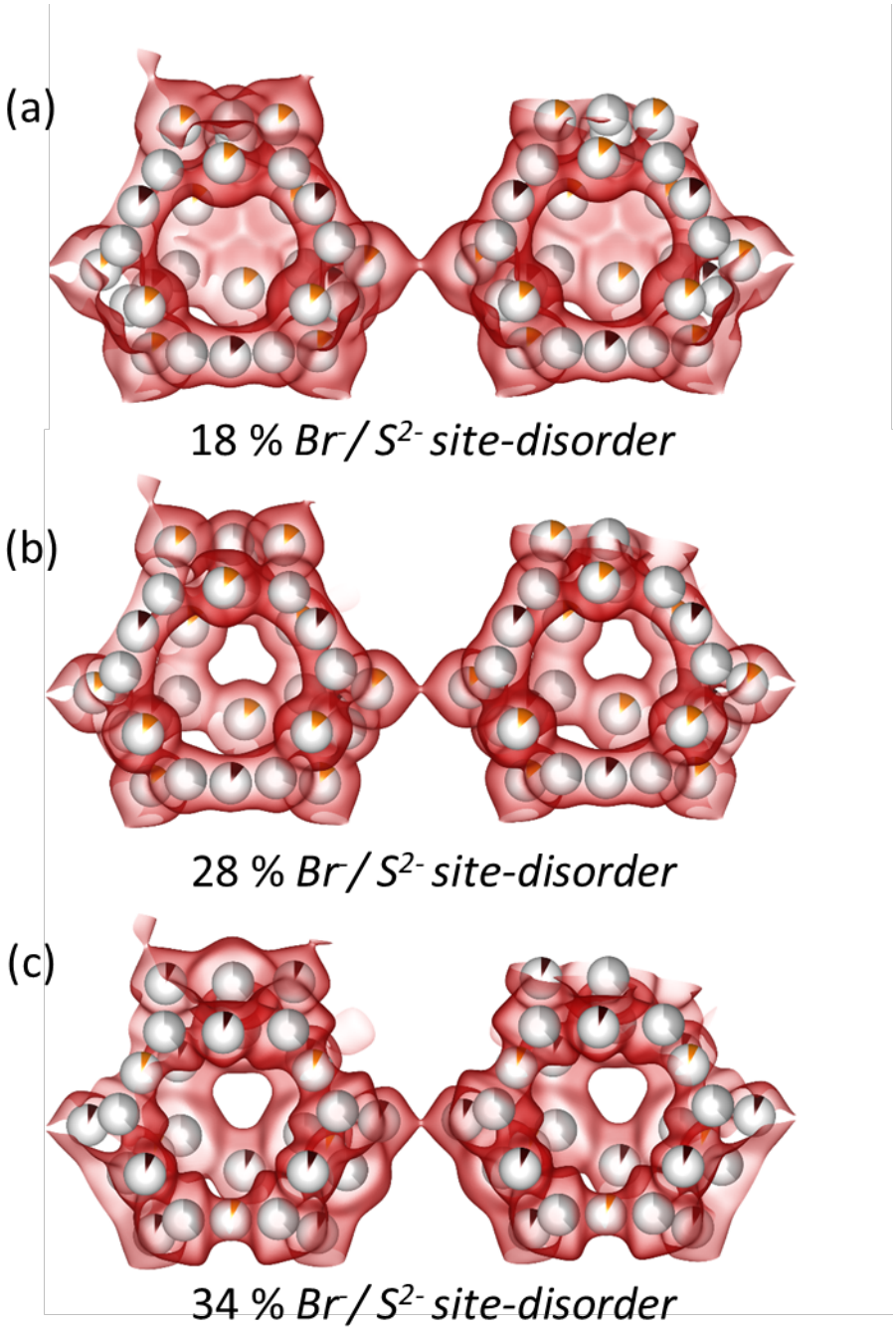

Figure S7: The Li-ion migration pathways were analyzed using the maximum entropy method (MEM). With increasing Br^-/S^{2-} site-disorder from (a) 18% to (b) 28% and (c) 34%, the Li^+ cage expands and larger R_{mean}, as well as shorter T2 – T2 sites, are found. (for each, two Li cages are illustrated, connected by the T2 – T2 bridge; all atoms except Li are removed for clarity)

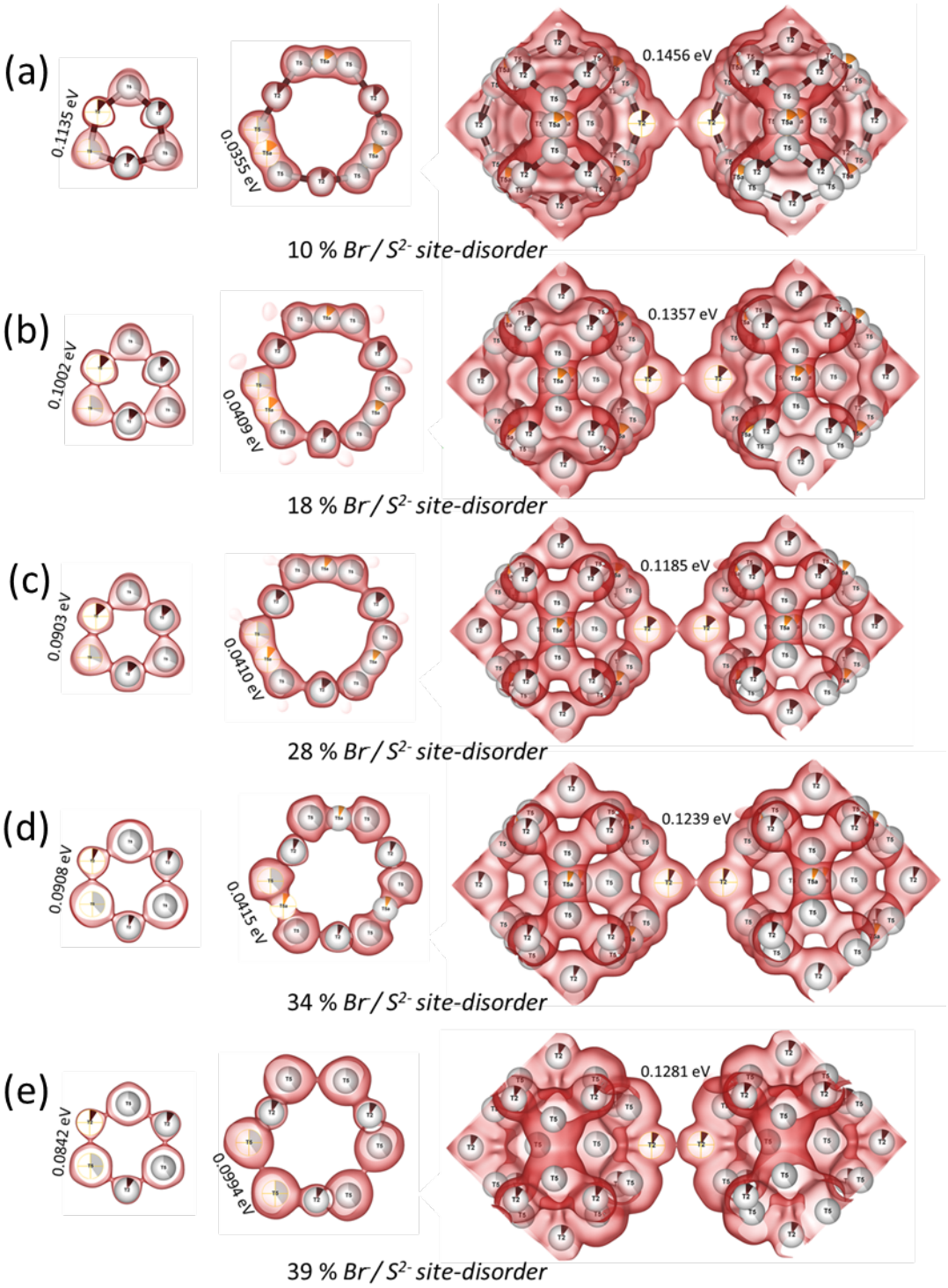

Figure S8: The Li-ion migration pathways were analyzed using the maximum entropy method (MEM). Representation of the Li^+ positions is denoted as T5 (Wyckoff 48h), T2 (Wyckoff 48h), and T5a (Wyckoff 24g). With increasing Br^-/S^{2-} site-disorder of (a) 10%, (b) 18%, (c) 28%, (d) 34%, and (e) 39%, the jump processes were described for a T5 – T2 distance, T5 – T5a distance and T2 – T2 distance., One-particle potential activation barriers are shown for selected distances.

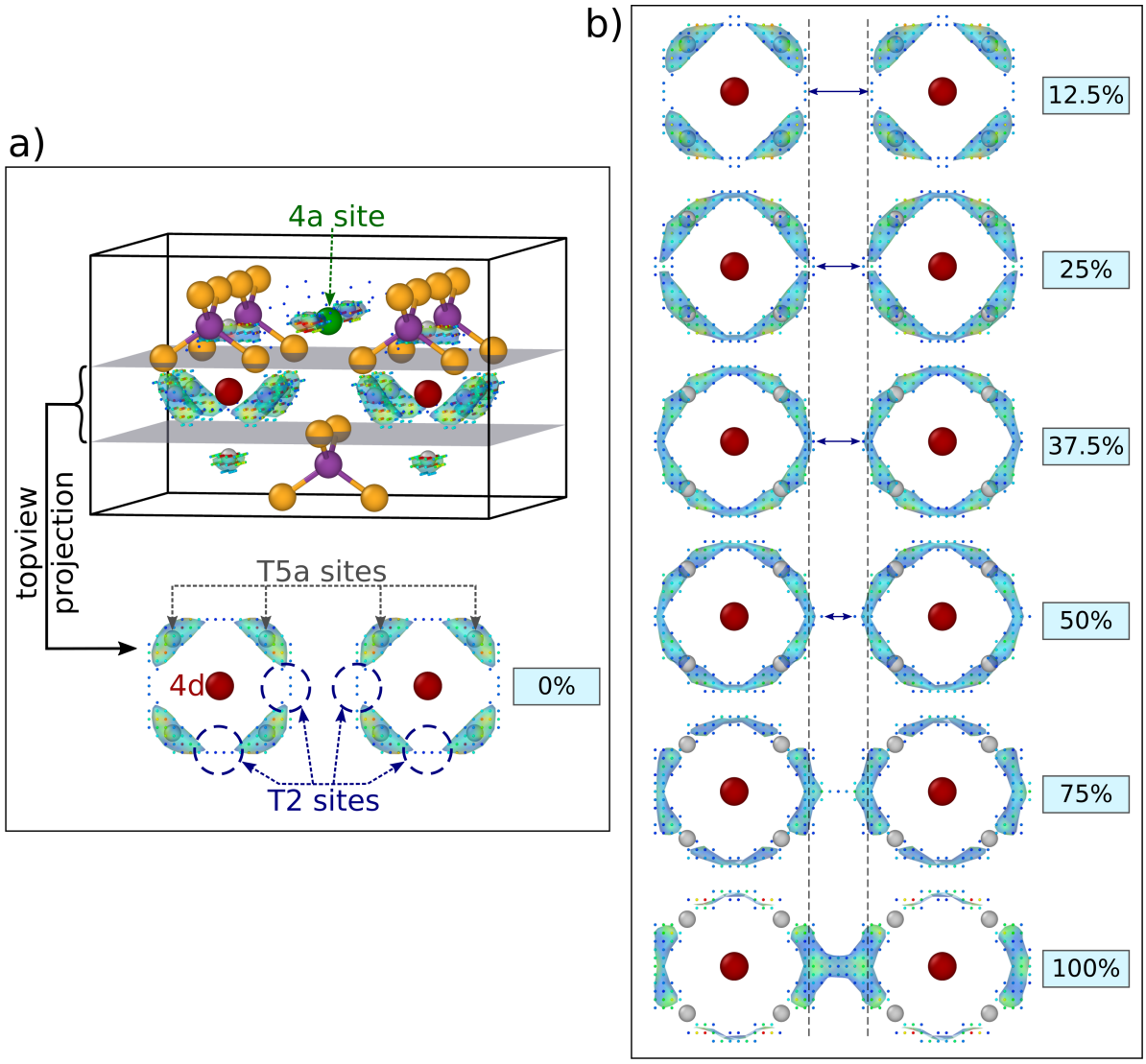

Figure S9: a) An atomistic model of two nominal 4d sites (large red spheres) and one nominal 4a site (large green sphere). The considerably smaller spheres represent the average Li probability density at 500 K. It has been obtained by averaging over the local Li probability densities of the simulated supercells and, similar to results obtained by diffraction data, it indicated the global average Li structure. Surface meshes have been added for better visualization. A top view projection of the region located between the two gray planes is visualized below the atomistic model for the structure with 0% Br^-/S^{2-} site-disorder. b) The respective top view projections for the different degrees of site-disorder. Gray spheres (approximate positions of the T5a sites), dashed lines and arrows indicating the T2-T2 distance are added as a guide to the eye. With increasing site-disorder the strong localization of Li on the T5-T5a-T5 sites starts to spread out until they form a network with the T2 sites. Simultaneously, the T2-T2 distance between neighboring cages decreases and the T5a sites become more and more shallow which breaks the network again for site-disorders above 50%.

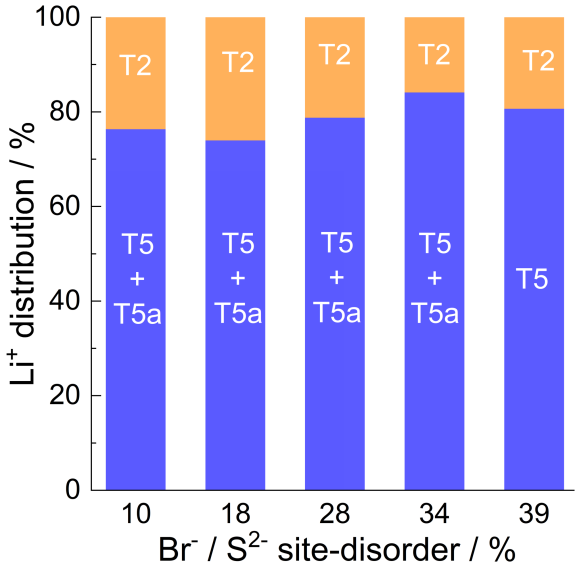

Figure S10: Li^+ distribution across the three sites T2 and (T5+T5a) over samples of increasing Br^-/S^{2-} site-disorder.

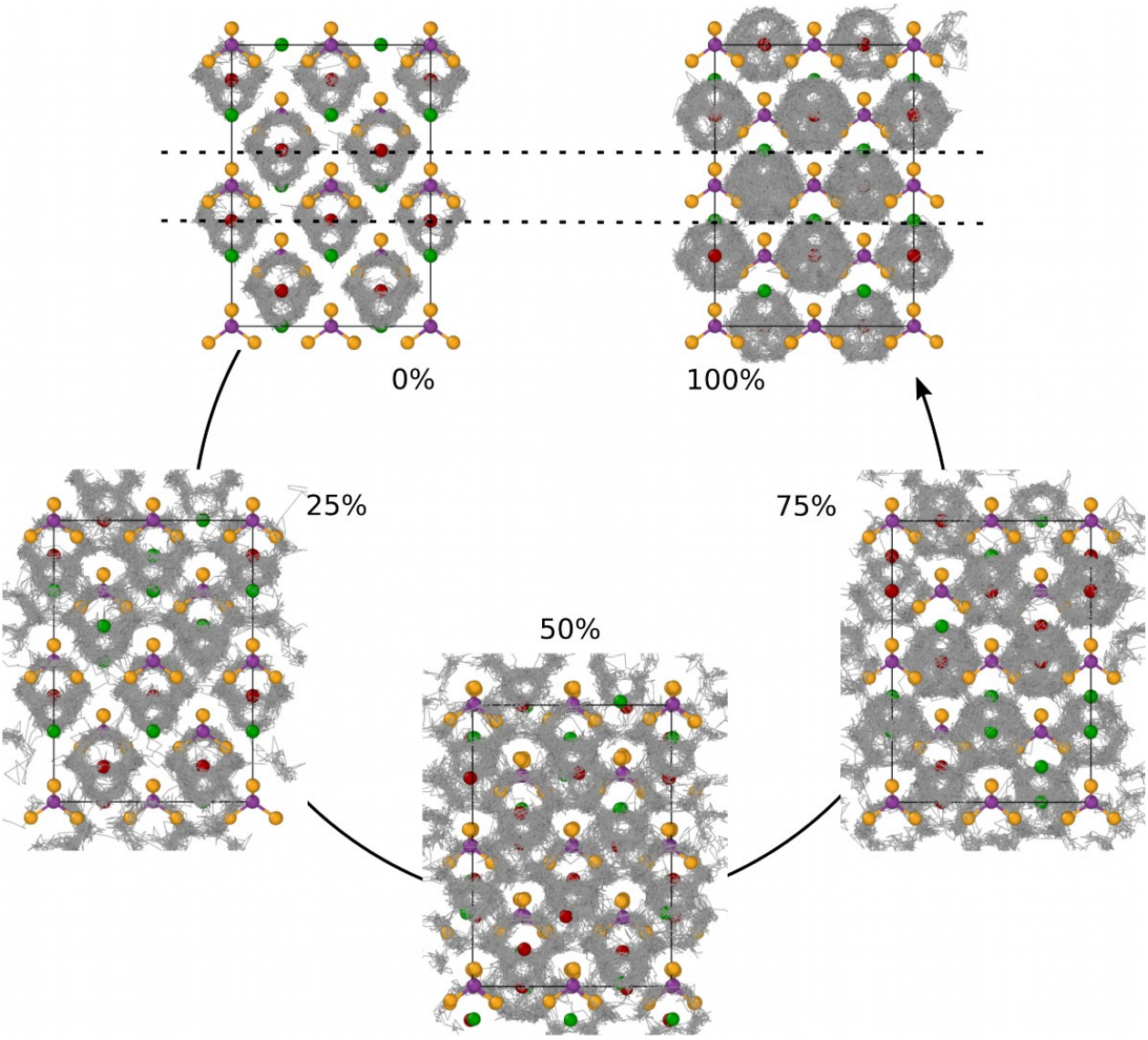

Figure S11: Exemplary Li trajectories (gray lines) for different degrees of site-disorder as labeled in the figure. The data were collected in AIMD simulations at 700 K for approximately 50 ps. With increasing site-disorder, the number of S^{2-} ions on the 4a sites increases and the Li cages are likewise shifted. Dashed lines are added as a guide to the eye in order to compare the cage positions.

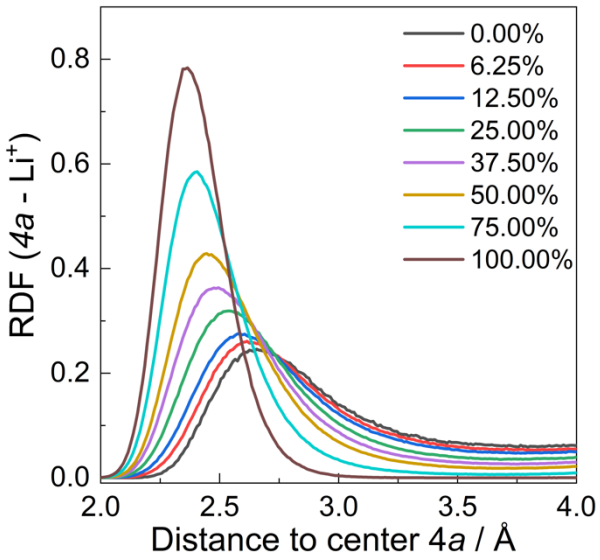

Figure S12: Calculated radial distribution functions of Li^+ with respect to the face centered anions Br^-/S^{2-} on 4a sites, as a function of site-disorder.

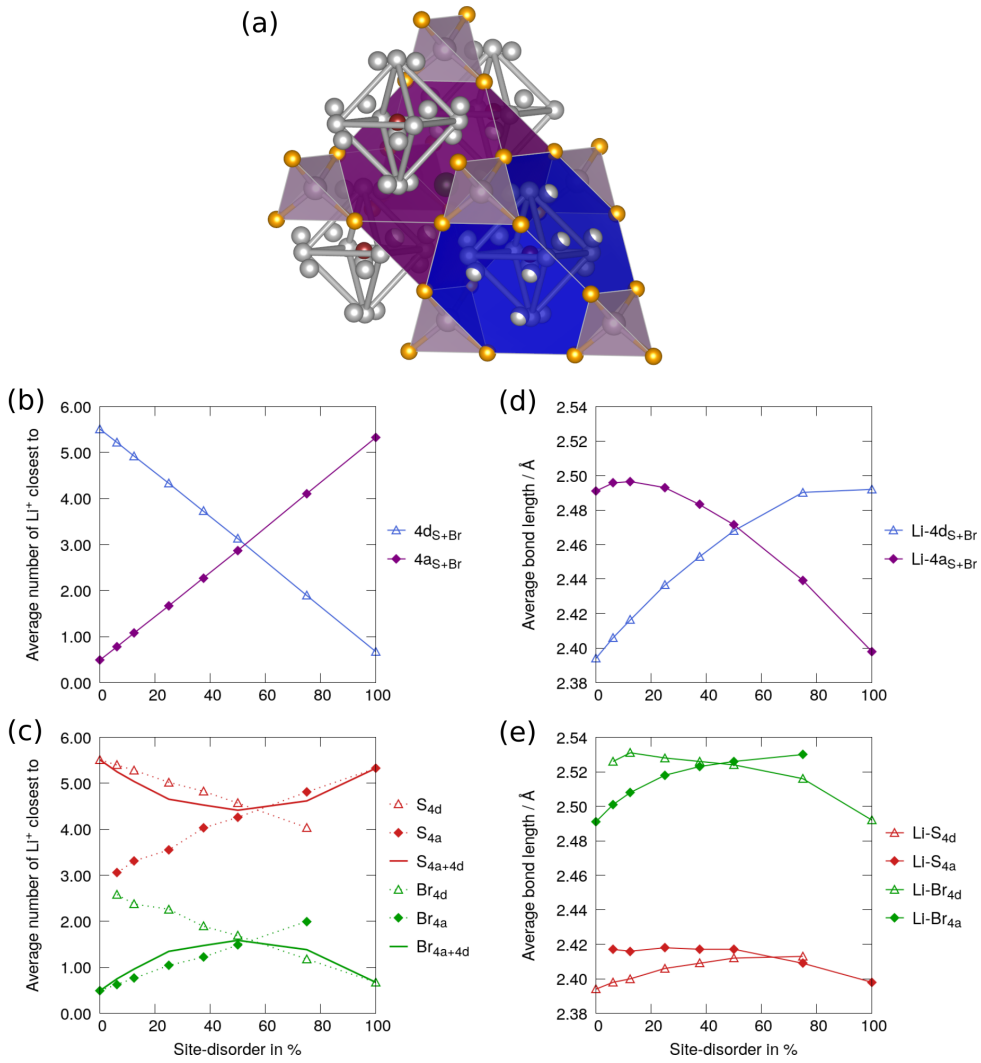

Figure S13: a) Coordination polyhedra that are spanned by the S ions of the PS_4^{3-} units around the central ion of the nominal tetrahedral 4d site (blue) and the nominal octahedral 4a site (deep purple). Based on the cell parameters used in the simulations the volume of the nominal octahedron V_O spanned by the P ions (181.35 Å^3) would be 4 times larger compared to the nominal volume of the tetrahedron V_T spanned by the P ions (45.33 Å^3). However, taking into account the S^{2-} ions of the PS_4^{3-} units as shown above adapts their volume. These coordination polyhedra are now of similar shape, which can be viewed as a tetrahedron truncated at their corners and approximately equal in volume (V_O=134.98 Å^3 and V_T=125.60 Å^3). Hence, the space to accommodate the central ion and the Li ions is roughly the same. In order to assign which Li ion resides in which polyhedron, we searched for their shortest bond length to the Br^-/S^{2-} ions on the 4a and 4d sites and classified it correspondingly. Therefore, each Li ion is only counted once. b) Average number of Li ions that are closest to the 4a and 4d site, irrespective if it is occupied by a Br^- or S^{2-} ion. In other words, it is the average number of Li ions residing in the respective polyhedra. In part c) this was broken down into the different contributions of Br^- and S^{2-}. Using only the above-mentioned shortest bonds the average bond length of the central atom to the Li ions belonging to the same cage has been calculated and shown in part d). The different contributions are shown in part e). The data were collected in AIMD simulations at 500 K.

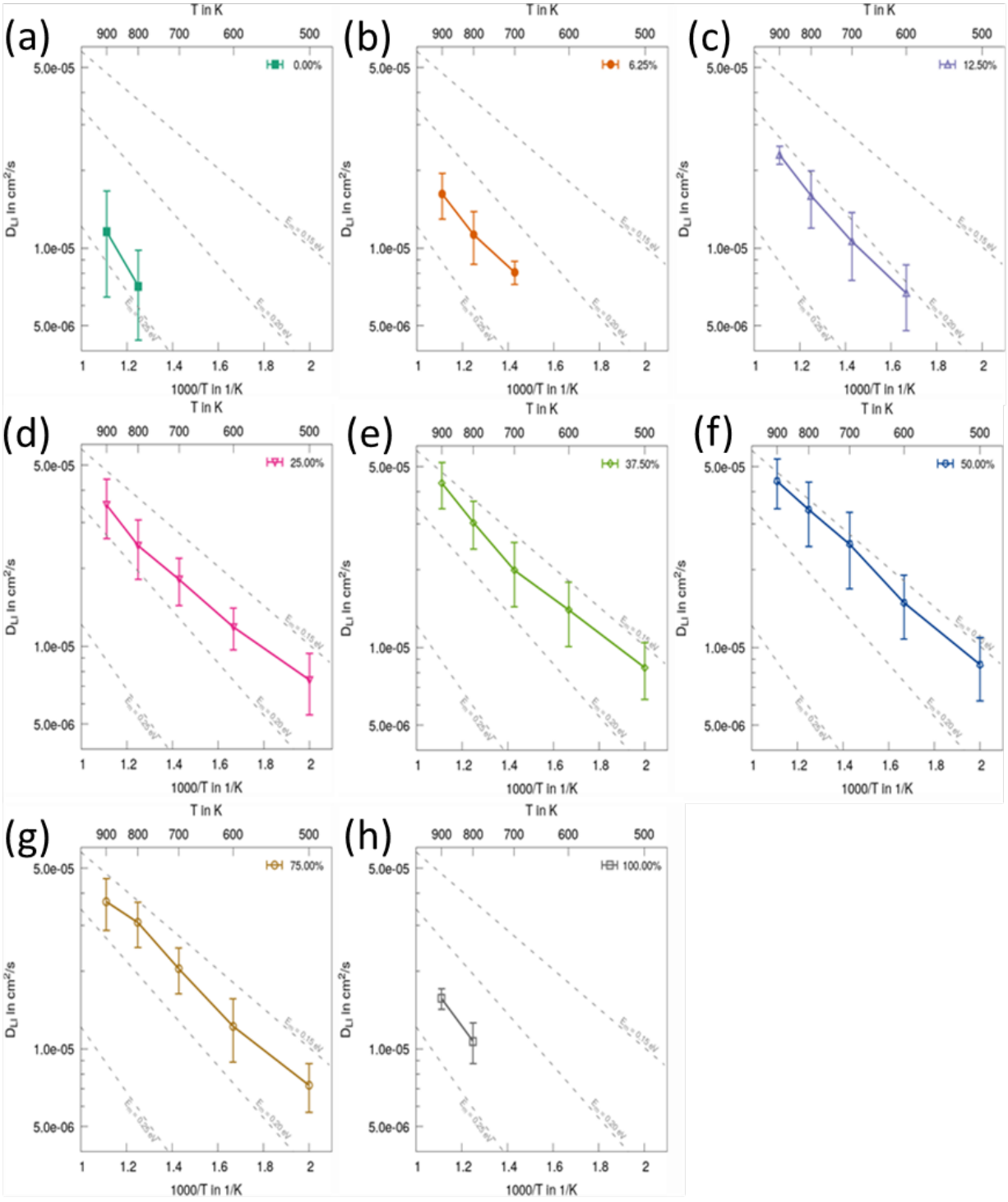

Figure S14: Calculated tracer diffusion coefficients as a function of temperature of various site-disorders (a) 0% (b) 6.25% (c) 12.5% (d) 25% (e) 37.5% (f) 50% (g) 75% (h) 100% together with Arrhenius fits according to $D_{Li}(T) = D_0 * \exp(-E_m/kT)$.

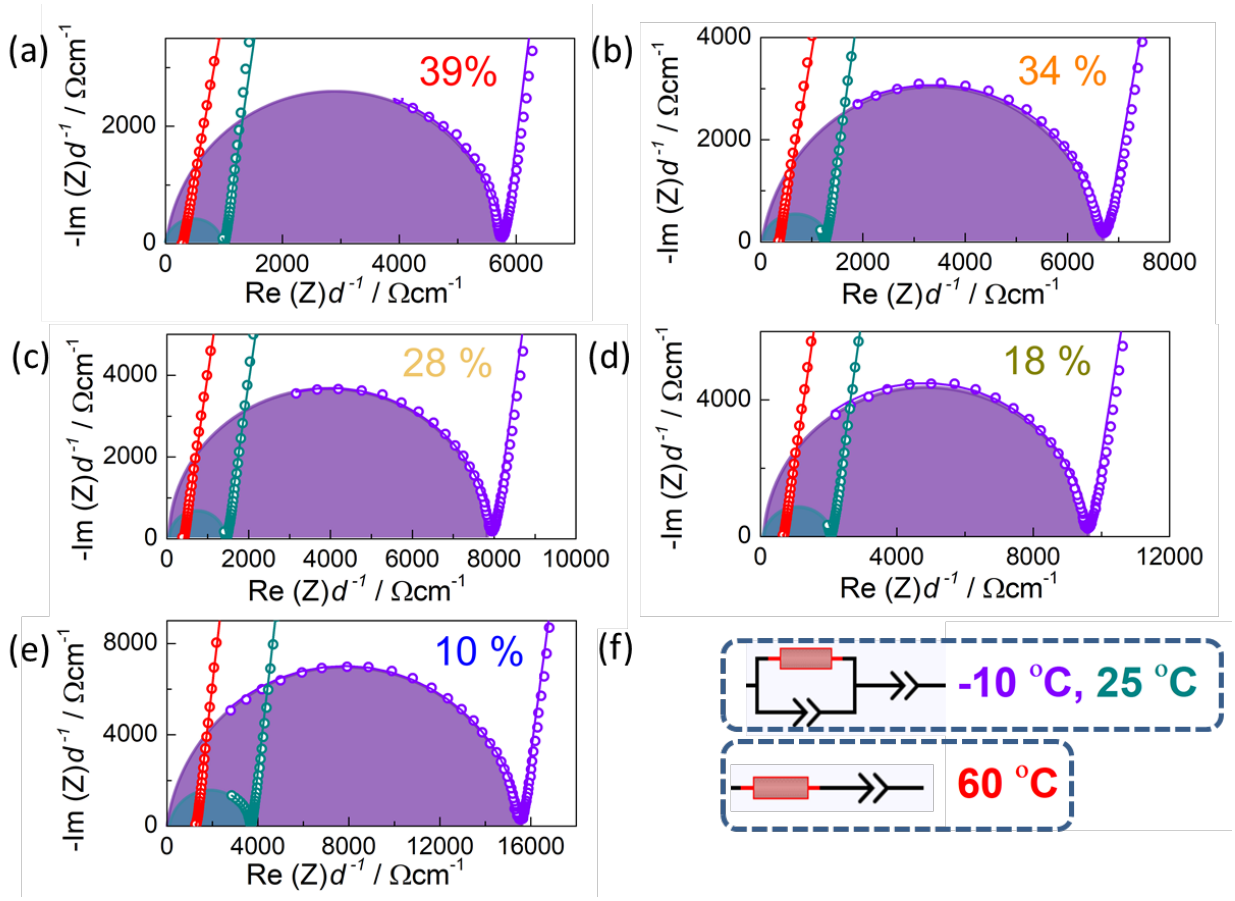

Figure S15: Representative fit of the impedance spectra of (a) 39%, (b) 34%, (c) 28%, (d) 18%, and (e) 10% measured with three different temperatures, (f) Impedance fit circuit at lower temperature and higher temperature

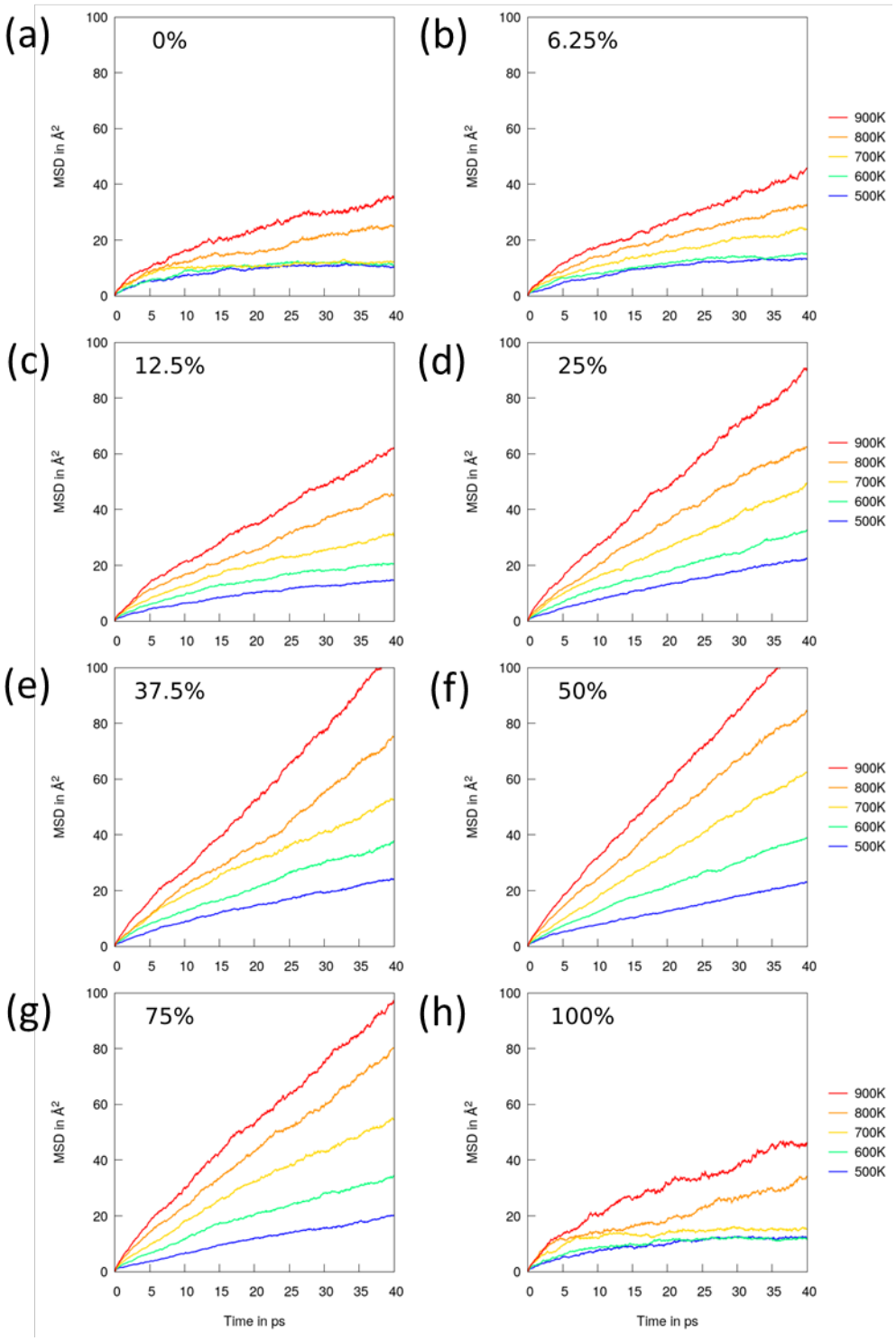

Figure S16: Mean-square displacement (MSD) Li^+ in a Li_6PS_5Br structure with increasing Br^-/S^{2-} site-disorder: (a) 0% (b) 6.25% (c) 12.5% (d) 25% (e) 37.5% (f) 50% (g) 75% (h) 100%.

References

(1) N. Minafra, M. Kraft, T. Bernges, C. Li, R. Schlem, B. J. M. W. G. Zeier, *Inorg. Chem.* **2020**, 59, 11009 - 11019.